

ULTRA HIGH SPEED AND HIGH TEMPORAL RESOLUTION DIAGNOSTICS IN GASEOUS DIELECTRICS

Pfeiffer, W.¹ and Schoen, D.²

¹ wpfeiff@hrz1.hrz.tu-darmstadt.de, TU Darmstadt, Germany

² schoen@hrzpub.tu-darmstadt.de, TU Darmstadt, Germany

ABSTRACT

This paper describes the application of a double frame camera system specially developed for investigation of high speed prebreakdown phenomena in compressed gases. Design principles and performance are presented in this paper.

INTRODUCTION

Ultra high speed photography in addition to electrical diagnostics are an important tool for spatial analysis of breakdown and prebreakdown phenomena in gaseous dielectrics [1,2]. The high temporal and spatial resolution capabilities of the camera system are discussed within this paper for selected examples in different gaseous dielectrics.

TEST VOLTAGE GENERATION

The test voltage is generated within a section of a coaxial gas insulated commercial bus duct. The test set-up includes a gas insulated bushing, a switching gap and a vessel with the test gap. As test voltage a very fast transient overvoltage (VFTO) was generated, because this voltage shape is known to be most critical for insulation properties under non homogeneous field conditions. Such field distribution may occur locally caused by protrusions or similar. Test peak voltages up to $V_{VFTO} = 600$ kV can be generated. Maximum gas pressure in the test vessel is $p = 0,9$ MPa. Within this paper oscillation frequencies of $f_{VFTO} = 10$ MHz and gas pressures up-to $p = 0,5$ MPa were applied and test voltages of $V_{VFTO} = 555$ kV have been generated. The test configuration is a slightly inhomogeneous (rowgowski profile) test gap with a needle shaped protrusion with a length of $l = 10$ mm. A high precision and hardened stainless steel needle with a curvature of $r_c = 0,5$ mm has been used. During the experiments described here, the gap width was $d = 30$ mm.

OPTICAL SET-UP AND CAMERA SYSTEM

To realise combined optical and electrical diagnostics of prebreakdown phenomena, the radiation of the prebreakdown phenomena has to be delayed by

several tens of nanoseconds. For this purpose the radiation of the prebreakdown phenomena was released from the test gap through an ultraviolet transparent glass windows towards a concave mirror which was installed at the distance l_1 . From there the image was projected along the length l_2 onto a small diameter focusing lens of the ultra high speed camera system, which was installed in the inner of a screened chamber. With this optical delay line a delay of $l_1 + l_2 = 55$ ns was achieved. Electro-optical investigations were realized with an total delay of $t_v = 25$ ns before the test gap was bridged by the prebreakdown phenomena, causing voltage collapse across the test gap. **Figure 1** shows the schematics of the ultra high speed and double frame camera system. All numbers in figure 1 are the delay time of the labelled parts. After passing a beam splitter, the luminous radiation is projected onto two separate image intensified camera systems. All lenses and mirrors of the camera system are optically corrected and made of UV transparent glass. Both intensified camera systems are double electronically gated multi microchannel plate intensifier tubes with CCD-Video-Adapter. The optical delay between both intensifier camera systems is zero. Maximum possible luminous gain is 81 dB for system I respectively 55 dB for system II. If breakdown occurs in the test gap, the current signal I_{VFTO} is used to trigger both camera systems separately. Most important for such an electronically triggered camera system is to keep the internal delay time as small as possible and to control problems due to electromagnetic interference caused by the high voltage transients. Special low propagation delay and multiple screened cables were used. Sophisticated triggering technique was used to guarantee stable triggering of both intensifier camera systems and to provide low jitter. For this purpose an avalanche transistorised trigger generator with low delay time was developed. If breakdown of the gaseous dielectric in the test gap occurred, the polarity of the triggering voltage is set to positive levels by the sub-nanosecond inverter and fed to the trigger generator. The trigger pulse from the trigger generator is split and fed to two separate, adjustable electronic delay lines. Trigger delay between two frames of an discharge event can be adjusted exactly for both intensifier camera systems. Temporal resolution of the delay line was 100 ps. In order to receive two precise time synchronous pulses for both camera triggering units of one intensifier camera system, the pulse from

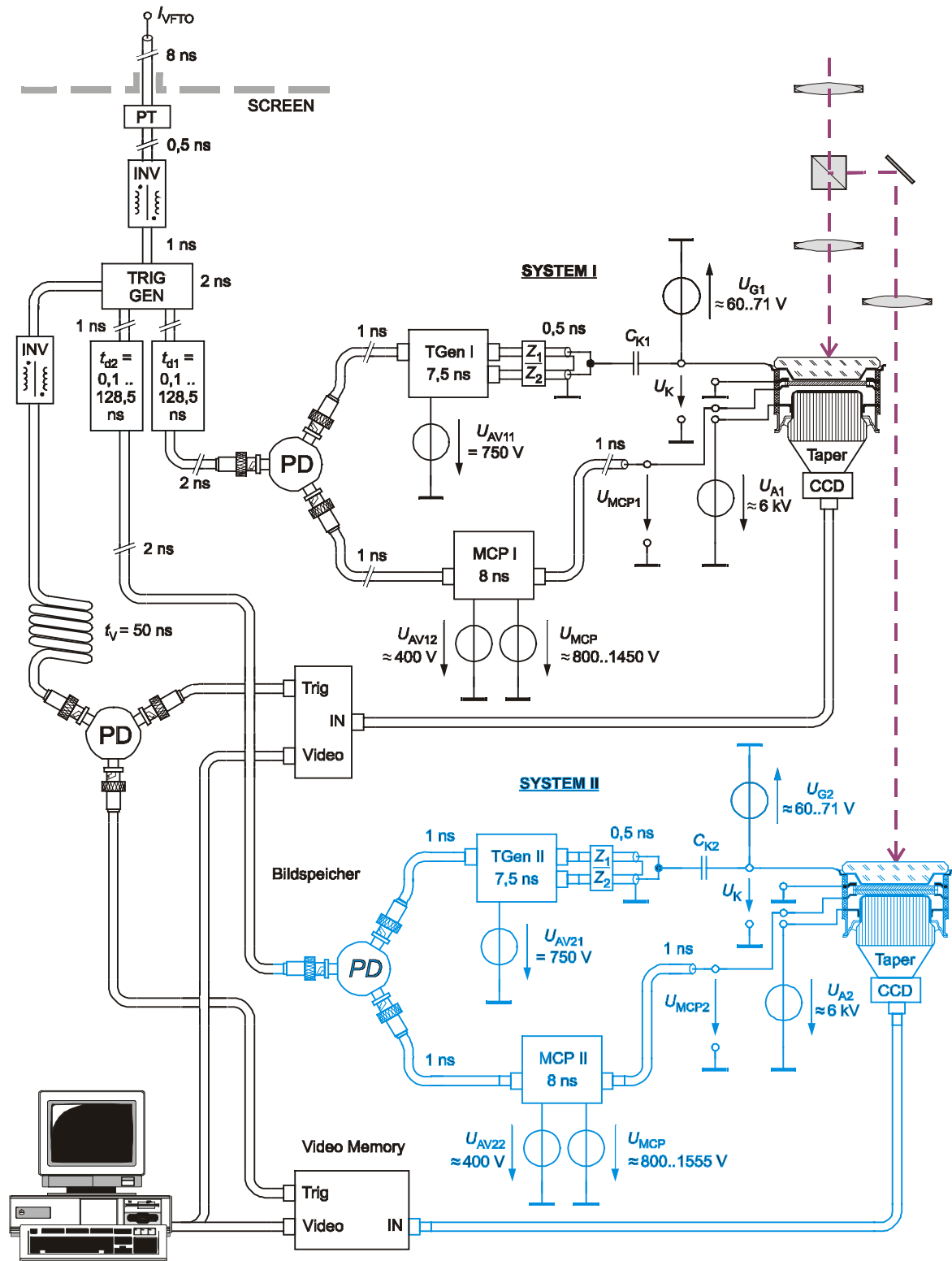


Figure. 1: Schematics of the double frame ultra high speed camera system

the delay line is split by a power divider. Both intensifier camera systems work in the same way. The following description is given for system I, but it refers also to system II. The first unit, TGen I, gates the photo cathode of the image intensifier. Gating times as low as $t_{ex} = 500$ ps are possible, $t_{ex} = 800$ ps were used within this paper. After having taken a

frame of the prebreakdown phenomena and closing the electronic shutter, the second unit, MCP I, switches off the gain of the image intensifier, to reject any light feed through of the image intensifier due to the very strong luminous radiation of the following spark. Both intensifier systems have to be synchronized carefully. Both pictures of the

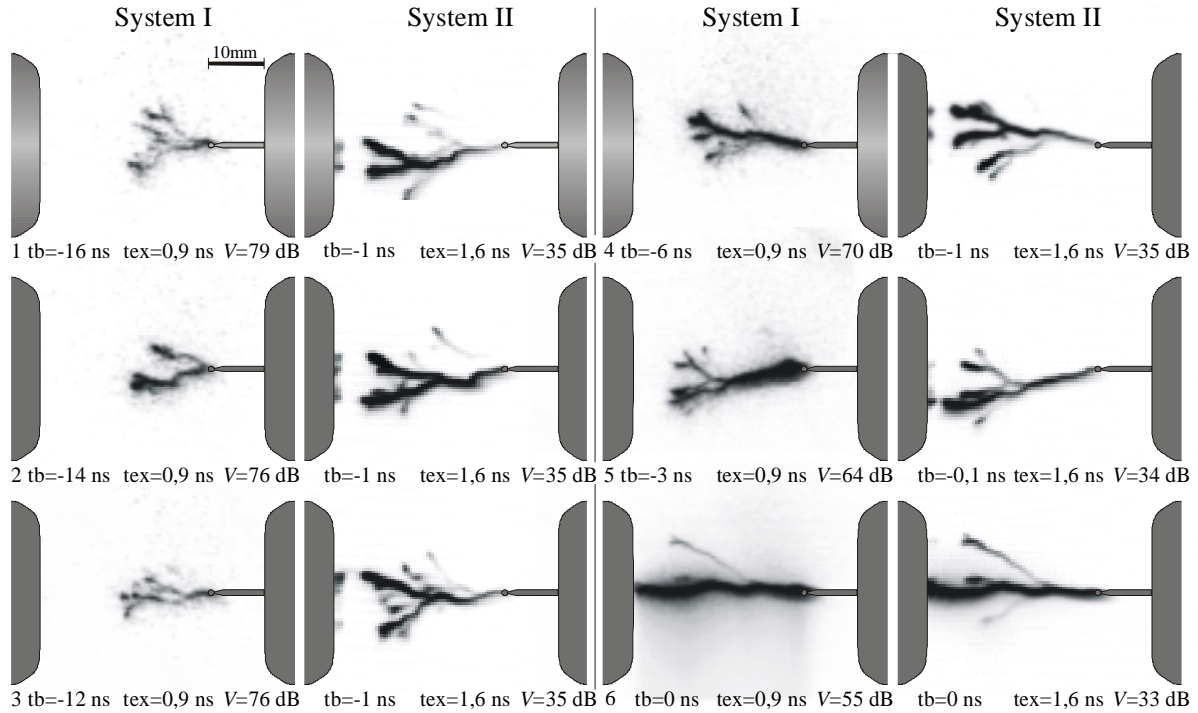


Figure. 2: Prebreakdown phenomena in SF_6 : $d = 30$ mm, $l = 10$ mm, $f_{VFTO} = 10$ MHz, $p = 0,5$ MPa.

prebreakdown phenomena on the phosphor screen of the intensified camera systems are fed by a conical taper to a peltier cooled CCD video chip. For the total optical integration time of the phosphor screen, both video signals are fed to a triggered high speed video memory. Then both frames of the prebreakdown phenomena are grabbed by a network connected computer system. As shown later, good reproducibility of the discharge phenomena at given experimental conditions can be guaranteed, so the sampling technique provides excellent information about the prebreakdown phenomena development in gaseous dielectrics.

APPLICATION OF THE HIGH SPEED CAMERA SYSTEM IN SF_6

Figure 2 shows first results which were obtained with the new double frame camera system. As during each prebreakdown development only two frames can be recorded (system I and system II), the whole prebreakdown phenomena must be reconstructed according to the before mentioned sampling technique. In **Figure 2** the last 16 ns of the spatial temporal development of the final jump in pure SF_6 at $f_{VFTO} = 10$ MHz are presented. While the time reference t_b to breakdown is nearly kept constant for system II, the delay time of system II was varied with the electronic delay line. By using this technique the spatial propagation of the prebreakdown phenomena can be observed seen and analysed clearly. When the prebreakdown phenomena reaches the plane cathode

area of the test gap (left side of **Figure 2**), the time reference t_b is set to zero for each experiment at different pressures. This is due to the changing magnitude of I_{VFTO} with pressure, hence the trigger levels for the trigger generator changes slightly, which on the other hand strongly effects the camera synchronisation to $t_b = 0$ ns. Numerous experiments were carried out for pure SF_6 using the new camera system. Only some results can be presented in this paper. Analysis of the prebreakdown phenomena in **figure 2** results in the following observations:

- Over the complete pressure range of $p = 0,0-0,9$ MPa and for all frequencies from $f_{VFTO} = 1-10$ MHz, avalanches starting from the cathode surface could be typically observed at the cathode plane (see **Figure 2**, picture 1 – 5, system II). This may be explained by the high field enhancement due to the highly conductive leader and the high dielectric strength of SF_6 .
- Compared to the prebreakdown development at $f_{VFTO} = 1$ MHz in SF_6 [10], the leader tips are spread more homogeneously and have higher luminosity at higher frequencies (see **Figure 2**, picture 1 – 3, 5, system II), especially for earlier stages of prebreakdown development. The spatial leader development is very similar to the stem-mechanism [3].
- For this pressure the average leader propagation velocity during the final jump can be estimated to $v_{L} = 0,76$ mm/ns. Average propagation velocities of the leader between $v_{L} = 0,70-0,76$ mm/ns have been

measured for pure SF₆ at 0,5 MPa and all frequencies between $f_{VFTO} = 1-10$ MHz.

- All experiments at f_{VFTO} larger than 1 MHz resulted in a higher dielectric strength of SF₆ for this configuration.. The energy mechanism [4] does not seem to be the only discharge mechanism. Rising dielectric strength between $f_{VFTO} = 1-15$ MHz was already reported before [5,6,7]. In contrast to this [8,9] report a reduction of the dielectric strength for f_{VFTO} greater than 10 MHz. Comparison of applied V_{VFTO} shape shows, that [8,9] applied a very weakly damped V_{VFTO} with nearly constant amplitude caused by a rising DC component. The test voltages V_{VFTO} applied in [8,9], and the V_{VFTO} voltages applied within

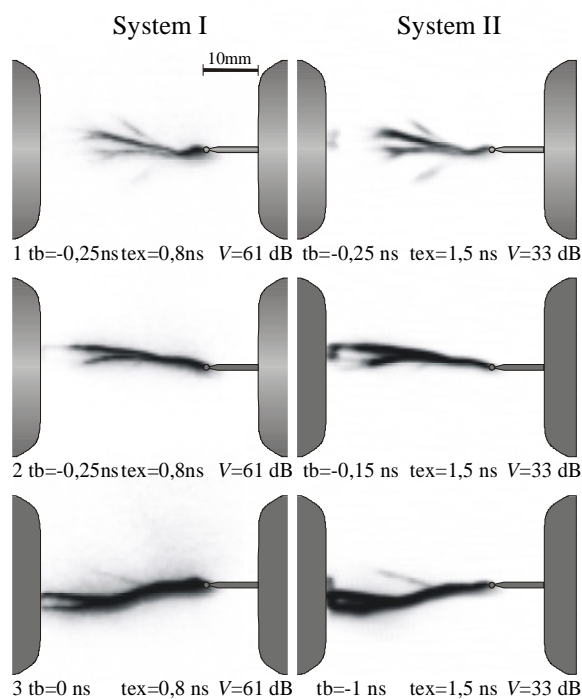


Figure. 3: Prebreakdown phenomena in an electronegative gas mixture; $d = 30$ mm, $l = 10$ mm, $f_{VFTO} = 10$ MHz, $p = 0,3$ MPa.

the performed experiments, always had a constant DC component and exponential damping of the amplitude, which was between 2.5 % (here) and up-to 10 % per oscillation [8,9]. Due to the high capacitive displacement current a rather uniform heating of the total critical volume may be a possible explanation for the higher dielectric strength at higher frequencies. On the other hand nearly constant V_{VFTO} amplitudes result in a rather long supply of high field strength and displacement current, which can reduce the dielectric strength for frequencies up to $f_{VFTO} = 15$ MHz.

REPRODUCIBILITY OF THE FRAMES

Figure 3 shows three different double frames of prebreakdown phenomena in an electronegative gas mixture. Time delay for intensifier system I is kept constant. Time delay of system II was shifted for

100 ps (picture 1 to 2) , respectively for 150 ps (picture 2 to 3). As can be seen, the very last jump of the leader is accelerated drastically. This behaviour is very typical for V_{VFTO} stress at $f_{VFTO} = 10$ MHz, respectively high frequency V_{VFTO} stress in electronegative gases. For smaller frequencies i. e. at $f_{VFTO} = 1$ MHz, the speed up of the very last jump of the leader endures up-to 1 ns. The speed up of the leader is due to the very high electrical field between cathode and anode. As can be seen from the first two frames of system II, field emission occurs at the cathode. The cathode material used was brass. The cathode surface had been polished carefully before carrying out the experiments. The picture series in figure 3 proves, that single or multiple framing series of the final jump are very good reproducible, as far as the experimental conditions are not changed. The high temporal reproducibility within the presented measurement could only be achieved with the new triggering technique described here. The jitter of the camera system is within the range of the temporal reproducibility. Differences of both intensifier camera systems in spatial resolution and luminous gain result from the use of two different types of image intensifier tubes.

CONCLUSIONS

A newly developed double frame camera system with gating times down to 500 ps is introduced. The importance of sophisticated camera triggering is emphasized. Some results obtained with the double frame camera system are presented in this paper. Spatial prebreakdown analysis indicates, that damping of the VFTO will influence the dielectric strength considerably.

REFERENCES

- [1] W. Pfeiffer, D. Schoen, C. Zender, "Dielectric Strength of SF₆/N₂ Mixtures for Nonuniform Field Distribution and Very Transient Voltage Stress" Int. Conference on Gas Discharges, Vol. 1, pp. 286 - 289, 1997
- [2] W. Pfeiffer, D. Schoen, C. Zender, "Corona Stabilization in SF₆/N₂ Mixtures under VFT Stress" ISH'99, pp. 3.84.S18 - 3.87.S18, 1991
- [3] L. Niemeyer, L. Ullrich, N. Wiegart, "The Mechanism of Leader Breakdown in Electronegative Gases" IEEE Trans. on Electrical Breakdown, Vol. 24 No. 2, pp. 309 - 324, 1989
- [4] D. Buchner, "Breakdown of SF₆ Insulation in Case of Inhomogeneous Fields under Different Transient Voltage Stress" ISH'95, pp. 2268-1 2268-4, 1989
- [5] W. Pfeiffer, V. Zimmer, P. Zipfl, "PredischARGE Development and Dielectric Strength of N₂, SF₆ and SF₆/N₂ Mixtures in Strong Non-Uniform Electrical Fields", ISH'91, paper 32.14, pp. 103 - 106, 1991
- [6] V. Zimmer, "Isolationseigenschaften von SF₆ und SF₆/N₂-Gemischen sowie von Stützisolatoren bei Beanspruchung mit hochfrequent oszillierender Stoßspannung", P. h. D-thesis, TU Darmstadt, 1994
- [7] C. Zender, "Möglichkeiten der Entladungsmesstechnik mit einem optimierten Kurzzeitkammersystem bei mit hochfrequent oszillierender Stoßspannung beanspruchten SF₆/N₂-Gasisolierungen", P. h. D-thesis, TU Darmstadt, 2001
- [8] H. Hiesinger "Statistical Time - Lag in Case of Very Fast Transient Breakdown" ISH'89, paper 32.23, pp. 1 - 4, 1989
- [9] S. Tenbohlen, "Der Einfluss dielektrischer Oberflächen auf die Durchschlagsentwicklung in einer störstellenbehafteten SF₆-Anordnung" P. h. D-thesis, RWTH Aachen, 1997
- [10] W. Boeck, W. Pfeiffer "Conduction and Breakdown in Gases" in the "Encyclopedia of Electrical and Electronics Engineering"; John Wiley; New York 2000.